Disulfide-Linked Allosteric Modulators for Multi-cycle Kinetic Control of DNA-Based Nanodevices

Erica Del Grosso, Irene Ponzo, Giulio Ragazzon, Leonard J. Prins, and Francesco Ricci*

Abstract: *Nature employs sulfur switches, that is, redox-active disulfides, to kinetically control biological pathways in a highly efficient and reversible way. Inspired by this mechanism, we describe herein a DNA-based synthetic nanodevice that acts as a sulfur switch and can be temporally controlled though redox regulation. To do this, we rationally designed disulfide DNA strands (modulators) that hybridize to a ligand-binding DNA nanodevice and act as redox-active allosteric regulators inducing the nanodevice to release or load its ligand. Upon reduction, the allosteric modulator spontaneously de-hybridizes from the nanodevice and, as a result, its effect is transient. The system is reversible and has an unprecedented high tolerance to waste products and displays transient behavior for over 40 cycles without significant loss of efficiency. Kinetic control of DNA-based ligand-binding nanodevices through purely chemical reactions paves the way for temporal regulation of more complex chemical pathways.*

Introduction

A strong current interest in the field of supramolecular chemistry is aimed at designing and synthetizing molecular devices that show features characteristic of living organisms like motility, adaptation, and evolution.[1] The possibility to create materials or devices that, for example, show temporal activation of functional properties, can lead to adaptable systems with unprecedented features.[2,3] A wide variety of dissipative systems, where the functionality of the synthetic device requires a constant supply of a high-energy chemical fuel for maintenance have been described to date.[4–8] The energy-dependence of the device functionality provides an efficient way to transiently activate or deactivate the material and its associated properties.[4,9] Many of these examples rely, like naturally occurring examples,[10–12] on the use of enzymes as fuel consuming units to return the system to its thermodynamic minimum.[13–16] However, recently, other approaches, based on purely chemical reactions that do not involve

biomolecular systems have been described.[8,14,17–28] These examples provide as main advantage the possibility to achieve a temporal control of the synthetic system in a more versatile and precise way without the drawbacks associated to enzymatic reactions like restricted experimental conditions, poor long term enzyme stability and enzyme inhibition by waste products.[29]

Recently, we and others have demonstrated that dissipative systems can be rationally designed using synthetic DNA sequences.[30–35] Compared to other molecules employed to date to achieve dissipative behaviour, DNA-based systems present a crucial advantage: thanks to the high programmability and predictability of DNA/DNA interactions it is in fact straightforward to control their thermodynamic energy landscape. The result are DNA devices that can be temporally controlled in a highly tunable and versatile way. To date, these systems have relied mostly on the use of DNA-recognizing enzymes as fuel consuming units. And while enzymes provide advantages for their selectivity towards specific DNA sequences, their use presents the limitations discussed above.

Motivated by the above arguments we demonstrate here the possibility to achieve temporal control of the binding activity of a DNA-based synthetic nanodevice in a reversible and highly controlled way through purely chemical reactions without the intervention of enzymatic systems. Our approach is inspired by Nature that employs redox reactions, and more specifically disulfide/thiol oxidation/reduction, to control biological pathways in different cellular environments (Figure 1a).[36–39]

Results and Discussion

To achieve redox-regulation over the binding activity of a DNA nanodevice, we rationally designed a DNA-based sulfur switch that can bind and release a ligand through oxidation/reduction cycles. To do this we selected as a model system a ligand-binding DNA-based nanodevice designed to adopt a stem-loop structure flanking two 18-nt tails at the two ends of the stem (Figure 1b). A single-stranded DNA sequence complementary to the loop portion of the nanodevice acts as the molecular ligand. We first envisioned a disulfide-linked dimer DNA strand that acts as a redox-active allosteric inhibitor (i.e. modulator). Such disulfide inhibitor is complementary to the two tails of the nanodevice (Figure 1b, grey strands). Binding of the disulfide inhibitor to the two tails of the nanodevice thus stabilizes the non-binding stem-loop structure and leads to the release of the ligand from the nanodevice. Such an allosteric effect critically relies on the integrity of the disulfide modulator. Upon reduction, the

[*] Dr. E. Del Grosso, I. Ponzo, Prof. F. Ricci
Department of Chemistry, University of Rome Tor Vergata
Via della Ricerca Scientifica 1, 00133 Rome (Italy)
E-mail: francesco.ricci@uniroma2.it

Dr. G. Ragazzon
Department of Chemical and Pharmaceutical Sciences, University of Trieste, Via L. Giorgieri 1, 34127 Trieste (Italy)

Prof. L. J. Prins
Department of Chemical Sciences, University of Padua,
Via Marzolo 1, 35131 Padua (Italy)

Supporting information and the ORCID identification number(s) for the author(s) of this article can be found under:
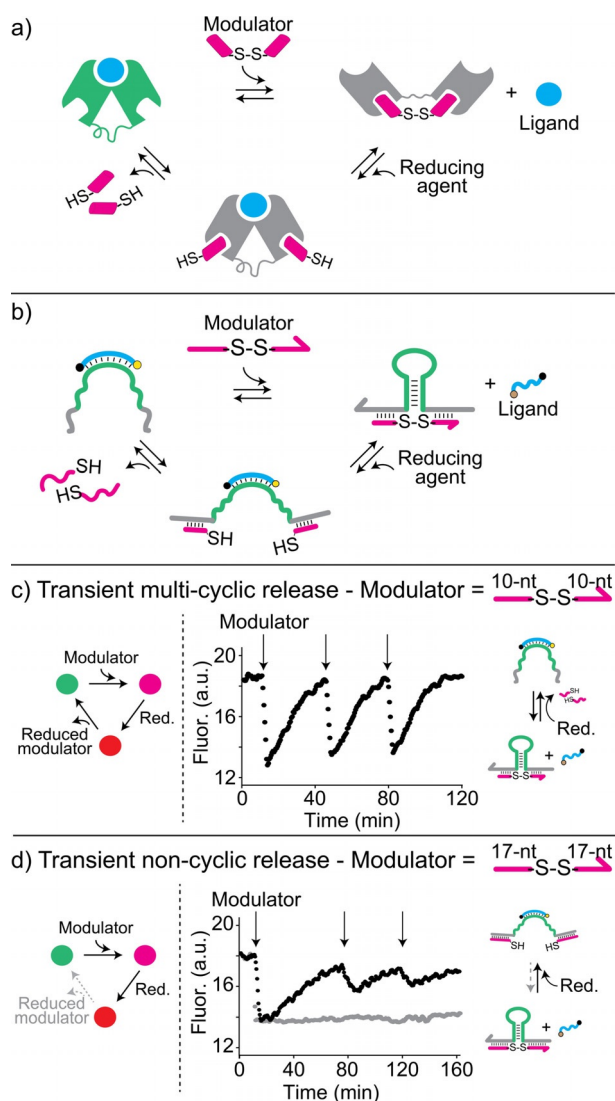https://doi.org/10.1002/anie.202008007.

Figure 1. a) Scheme of redox-controlled ligand binding: a redox-responsive modulator (red) acts as a transient allosteric inhibitor for a ligand-binding receptor (grey). b) DNA-based nanodevice controlled by redox inputs. The nanodevice is designed as a stem-loop flanking two tails (grey portions, allosteric sites) and binds a DNA ligand (blue strand) complementary to the loop. A DNA disulfide modulator strand hybridizing to the two tails stabilizes the stem-loop non-binding conformation leading to the release of the ligand. Once reduced, the two thiolated halves of the modulator spontaneously de-hybridize from the nanodevice. c) Transient multi-cyclic release: the disulfide inhibitor, once reduced, spontaneously de-hybridizes from the nanodevice and allows multiple transient cycles. d) Transient non-cyclic release (black curve): the thiolated reduced portions of the inhibitor remain bound to the nanodevice after the first redox transient cycle and this hinders efficient successive cycles. Non-transient release (grey curve): a non-redox inhibitor (lacking the disulfide bond) binds to the tails of a stem-loop nanodevice and triggers the permanent release of the ligand. Kinetics traces were obtained in a 100 mM Tris-HCl, 150 mM NaCl, 10 mM MgCl$_2$, TCEP 5×10^{-4} M solution, pH 8.5, at 45 °C in the presence of the ligand (3×10^{-8} M) and the DNA nanodevice (5×10^{-8} M) and upon the addition of the inhibitor (5×10^{-7} M).

reduced thiolated portions (here defined as waste products) of the inhibitor would not be able to stabilize the non-binding loop: as a result, the allosteric effect will be transient and the

binding ability of the nanodevice restored over time (Figure 1b). Additionally, the disulfide modulator should be designed so that, once reduced, the two halves would spontaneously de-hybridize from the nanodevice, allowing new transient load/release cycles.

We have rationally designed a DNA allosteric modulator/inhibitor that meets the outlined requirements by employing simulation (Nupack) and binding affinity data. Our design was also facilitated by previous observations obtained with disulfide DNA controllers employed for the temporal control of nanotube self-assembly.[40] The allosteric inhibitor is composed of two 10-nt portions complementary to the two tails of the nanodevice linked by a disulfide bond (Figure 1b). The complete disulfide inhibitor (20-nt) shows a strong affinity for the nanodevice ($K_D = 4.1 \pm 0.2 \times 10^{-8}$ M, Figure S1) so that efficient hybridization of the oxidized inhibitor to the nanodevice could be observed. The reduced inhibitor portions (i.e. the 10-nt thiolated halves), in contrast, show a much poorer affinity for the nanodevice ($K_D = 1.4 \pm 0.3 \times 10^{-5}$ M) so that rapid de-hybridization occurs when the inhibitor is reduced (Figure S2).

The above described allosteric disulfide inhibitor allows multi-cycle transient control of ligand release through redox inputs. To follow the ligand's loading/release from the nanodevice we have labelled the DNA ligand with a fluorophore and quencher pair, so that the association of the ligand to the nanodevice is accompanied by an increase in fluorescence intensity while its release results in a decrease of the signal. The addition of the disulfide inhibitor to a solution containing the nanodevice/ligand complex and a reducing agent (here tris(2-carboxyethyl)phosphine, TCEP) leads to the rapid release of the ligand from the nanodevice as demonstrated by the fluorescence signal decrease (Figure 1c). This is due to the fact that the disulfide inhibitor hybridization to the two tails of the nanodevice stabilizes the non-binding state of the nanodevice shifting its apparent binding affinity for the ligand to higher concentrations (i.e. from $5.4 \pm 0.1 \times 10^{-8}$ M to $6.7 \pm 0.5 \times 10^{-7}$, see Figure S3). Upon reduction of the disulfide bond the inhibitor is split into its two 10-nt thiolated halves and its effect on the stabilization of the non-binding conformation of the nanodevice is suppressed over time. The nanodevice thus restores its original binding ability (Figure S4) and the ligand is gradually re-loaded (Figure 1c). Of note, the affinity of the 10-nt reduced halves of the inhibitor for their complementary portions is so poor that, under the experimental conditions employed, they spontaneously de-hybridize from the nanodevice. For this reason, multiple load/release cycles with comparable efficiency can be achieved upon new successive additions of the disulfide inhibitor (Figure 1c). As expected, when the same experiment is carried out in the absence of the reducing agent the disulfide inhibitor leads to a permanent release of the ligand (Figure S5).

To further support the proposed mechanism, we have also performed control experiments using a longer inhibitor (i.e. total length, 34 nt) and an inhibitor lacking the disulfide bond. In the first case (Figure 1d, black curve) we have observed the same transient behaviour upon reduction of the disulfide bond. However, because the affinity of the two 17-nt thiolated

halves of this inhibitor for their complementary portions is high (Figure S6) they remain bound to the nanodevice and the system does not allow efficient successive transient cycles. In the second control experiment, the inhibitor lacks the disulfide bond and leads to a non-transient permanent release of the ligand from the DNA nanodevice. The activity of this inhibitor is in fact not affected by the presence of the reducing agent in solution and its effect is stable over the entire course of the experiment (Figure 1 d, grey curve).

The transient redox-controlled process is highly tolerant and presents minimal inhibition effect due to waste products. Indeed, we performed multiple load-release cycles through successive additions of the 20-nt redox inhibitor to a solution containing the reducing agent and the nanodevice/ligand complex (Figure 2 a). The system displays transient behaviour for up to forty complete cycles without a significant loss of efficiency in ligand-reloading kinetic. The half-life of redox-controlled reloading, in fact, remains constant and does not show any sign of delay (Figure 2 b).

To gain a more complete insight into the kinetic processes involved and to better understand the signal profile of the system, a kinetic model was developed and used to fit the multiple load-release cycles (Figure 2 a, red line). The system was described by a reaction network in which waste interference occurs upon binding of the waste to the unbound device, as well as the device-ligand complex (see SI and Figure S7 for more details). Introduction of waste interference was key to reproduce the observed behaviour. Indeed, the loss of fluorescence intensity observed over time is due to the high concentration of waste products produced after many cycles

(for example 1.5×10^{-5} M of waste products is produced after 15 cycles). At this high concentration even the low-affinity 10-nt thiolated halves remain partially bound to the nanodevice, causing a loss of efficiency. Moreover, accumulation of the complex between the device and the thiolated waste product accounts also for the drift in emission intensity, as confirmed by independent experiments showing that the emission intensity of such inactive complex is higher than that of the free-standing nanodevice (Figure S2).

To further strengthen the validity of the proposed model, the same kinetic Scheme was used to model the operation of the system with the longer (34-nt) inhibitor that leads to a transient non-cyclic behaviour (Figure 1 d and S8). Also in this case, the model is able to reproduce the experimental data. Here, the interference of the waste product is much more pronounced as the affinity between the thiolated halves of the inhibitor and the nanodevice is higher ($K_D = 1.6 \pm 0.1 \times 10^{-8}$ M). The species involving the waste product become dominant already after the first cycle, with a complete depletion of the binary device-ligand complex. As a consequence of this, in the second and third cycle, the ligand release occurs from a ternary complex involving device, ligand and waste.

We can finely regulate the transient control of the binding efficiency of a DNA-based nanodevice using redox reactions. To demonstrate this, we have controlled the time interval with which the DNA ligand is re-loaded by the nanodevice by varying the concentration of both the disulfide modulator and the reducing agent. The half-life for ligand re-loading, for example, can be increased from 12.0 to 20.8 minutes upon increasing the disulfide inhibitor concentration from 3×10^{-9} to 1×10^{-6} M at a fixed concentration of the reducing agent (TCEP at 5×10^{-4} M) (Figure 3 a). Alternatively, it is also possible to finely regulate the re-loading process, by using different concentrations of the reducing agent (from 1 to 500×10^{-6} M) and at a fixed concentration of the disulfide inhibitor (5×10^{-7} M). By doing so we regulated the re-loading half-life from 217 to 17 minutes, respectively (Figure 3 b). Finally, because the disulfide reduction reaction is strongly pH-dependent, we can also regulate the transient release by varying the pH at which the experiment is carried out (Figure S9). By doing so we can modulate the half-life for ligand re-loading from 193 to 17 minutes by varying the pH from 6.5 to 8.5, respectively. We also investigated the possibility of using different reducing agents including two that are more biologically relevant (i.e cysteine and gluta-thione) obtaining similar results in terms of transient behaviour and response time (Figure S10).

To demonstrate the versatility of our approach we have also re-engineered the DNA-based nanodevice so that we can kinetically control the binding rather than the release of the ligand. To do this we have designed a disulfide modulator/activator that binds to only one of the two tails of the nanodevice and partially invades the stem thus destabilizing the non-binding structure of the nanodevice (Figure 4 a, S11). This DNA modulator thus acts as an allosteric activator that improves the affinity of the nanodevice for the ligand (Figure 4 b, curve green). Also in this case, upon reduction, the disulfide activator looses its functionality and the original
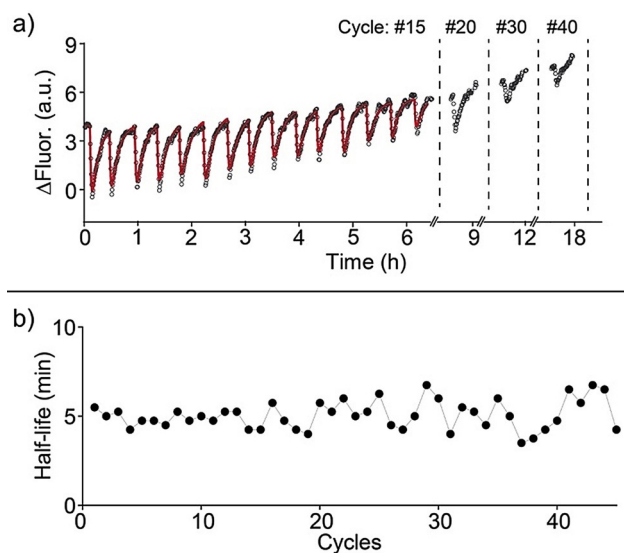

Figure 2. a) Kinetic traces showing the transient release of the ligand from the nanodevice after sequential addition of the disulfide inhibitor strand (20-nt) in the presence of a constant concentration of reducing agent (TCEP); the solid red line represents the fitting according to the presented kinetic model (see text and SI). b) Half-life of ligand release for each transient cycle. Experiments were performed in a 100 mM Tris-HCl, 150 mM NaCl, 10 mM MgCl$_2$, TCEP 5×10^{-4} M solution, pH 8.5, at 45 °C in the presence of the ligand (5×10^{-8} M) and the DNA nanodevice (5×10^{-8} M) and upon the addition of the disulfide inhibitor (5×10^{-7} M).
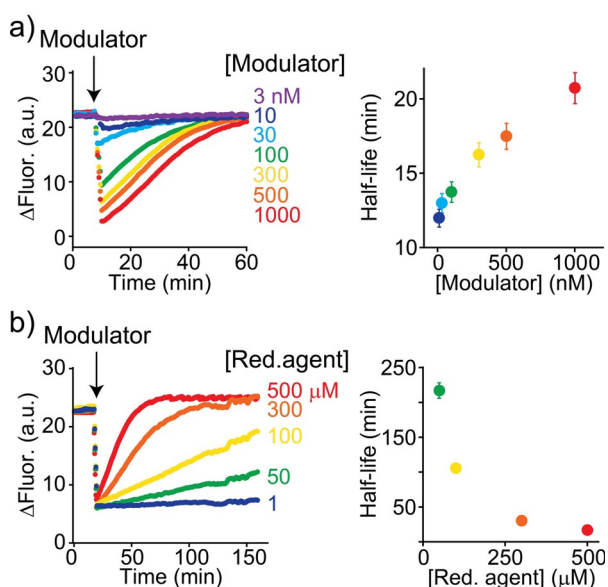
Figure 3. Kinetic traces showing the transient release of the ligand from the nanodevice at different concentrations of the a) disulfide modulator inhibitor (20-nt) and b) the reducing agent (TCEP). Half-lives of ligand release for each transient cycle are also plotted against (a) modulator and (b) reducing agent concentration. Experiments were performed in a 100 mM Tris-HCl, 150 mM NaCl, 10 mM MgCl$_2$ solution, pH 8.5, at 45°C in the presence of the ligand (3×10^{-8} M) and the DNA nanodevice (5×10^{-8} M). In (a), a fixed concentration of reducing agent was used (TCEP 5×10^{-4} M) while in (b) a fixed concentration of disulfide inhibitor was added (5×10^{-7} M). Error bars represent standard deviation based on triplicate measurements.

affinity towards the ligand is restored (Figure 4b, curve red). The addition of such disulfide DNA activator would thus trigger the transient loading of the ligand to the nanodevice and, upon reduction, the ligand would be gradually re-released over time (Figure 4c). Because in the reduced form

the two 10-nt halves of the modulator are spontaneously released from the nanodevice, successive additions of the activator allow to achieve efficient multiple load/release cycles (Figure 4c).

To substantiate the observed behaviour, a kinetic model was used to fit the experimental data (Figure 4c, red line, see SI and Figure S12 for details). The prominent feature of the model is a cyclic reaction network in which the activator binds to the nanodevice, allowing the subsequent binding of the ligand. Upon reduction of the disulfide, the waste products are de-hybridized, followed by a gradual release of the ligand. Importantly, the system is operated with a low concentration of activator (i.e. 1×10^{-7} M), which limits waste interference. Still, the influence of the waste products is evident from the progressive decrease in emission intensity of each end-cycle plateau. As demonstrated with the first system, also in this case the life time of the disulfide modulator can be modulated by varying its concentration. More specifically, the half-life changed from 6.5 to 14.5 minutes upon increasing the disulfide activator concentration from 3×10^{-8} to 1×10^{-7} M at a fixed concentration of the reducing agent (TCEP, 5×10^{-4} M) (Figure S13).

Alternatively, it is also possible to finely regulate the transient loading process, by using different concentrations of the reducing agent (from 1×10^{-6} to 1×10^{-3} M) and at a fixed concentration of the disulfide activator (1×10^{-7} M) (Figure S14).

A major feature of naturally-occurring sulfur switches[41] is that they are highly reversible and through oxidation/reduction cycles their activity can be easily controlled. We have thus attempted to demonstrate a similar redox-reversibility for our DNA-based systems. To do this we have initially employed the DNA nanodevice controlled by the longer disulfide inhibitor (34-nt) (Figure 1d). As expected, the addition of a reducing agent (here TCEP) to a solution containing the nanodevice/inhibitor complex induces the
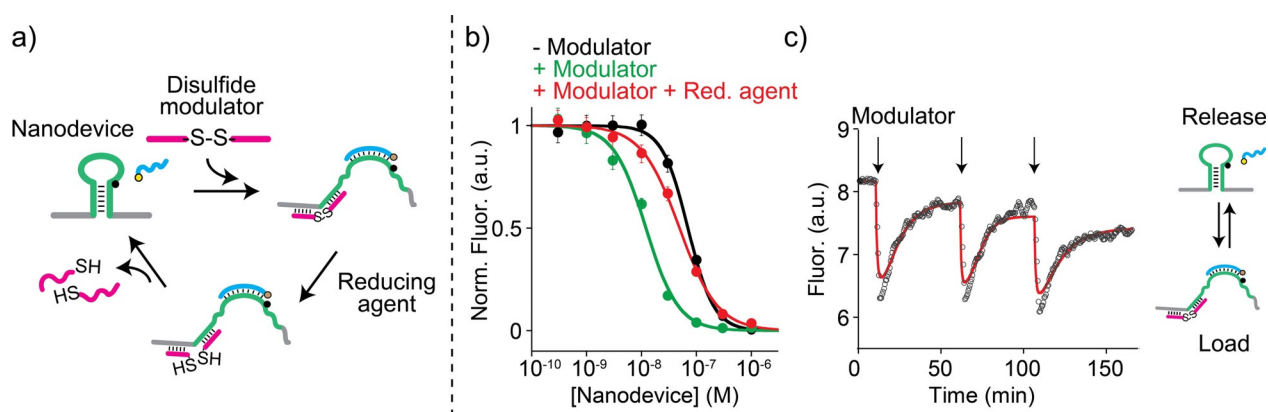

Figure 4. a) A stem-loop nanodevice (green strand) is allosterically controlled by a disulfide modulator (purple strand) that acts as an allosteric activator. b) Binding curves of the nanodevice/ligand interaction in the absence (black) and presence (green) of the disulfide modulator activator. The binding curve in the presence of the disulfide activator and the reducing agent is also shown (red). c) Kinetic traces showing the transient loading of the ligand (3×10^{-8} M) by the nanodevice (1×10^{-8} M) upon addition of the disulfide activator (1×10^{-7} M). The reduced portions of the activator are spontaneously released from the nanodevice and thus the effect is reversible upon new addition of the modulator; the solid red line represents the fitting according to the presented kinetic model (see text and SI). Experiments were performed in 100 mM Tris-HCl, 150 mM NaCl, 10 mM MgCl$_2$ solution, pH 8.5, at 45°C. Binding curves have been obtained at a fixed concentration of ligand (3×10^{-8} M) and, where indicated, in the presence of activator (1×10^{-7} M) and TCEP (1×10^{-3} M). Error bars represent standard deviation based on triplicate measurements.

loading of the ligand by the nanodevice. The following addition of the oxidizing agent (here H_2O_2), leads to a signal decrease, suggesting that the reduced inhibitor is re-oxidized and the ligand released, although with a slightly reduced efficiency (Figure 5a). The nanodevice binding affinity for the ligand after the oxidation reaction is, at $3.5 \pm 0.5 \times 10^{-7}$ M, similar to that observed before reduction $(5 \pm 1 \times 10^{-7}$ M) (Figure S15) thus supporting the hypothesis that re-oxidation of the disulfide modulator restores its inhibitor activity. A similar reversibility experiment was also performed using the nanodevice controlled by the disulfide activator characterized above (Figure 4). The addition of the reducing agent to a solution containing the nanodevice/activator complex induces the release of the ligand from the nanodevice as demonstrated by the fluorescence signal decrease. The addition of the oxidizing agent to this solution leads to a signal increase, indicating the loading of the ligand and thus suggesting re-oxidation of the activator (Figure 5b). To confirm this, the nanodevice binding affinity for the ligand after the oxidation reaction is, at $2.7 \pm 0.4 \times 10^{-8}$ M, similar to that observed before reduction $(2.6 \pm 0.7 \times 10^{-8}$ M) (Figure S16).
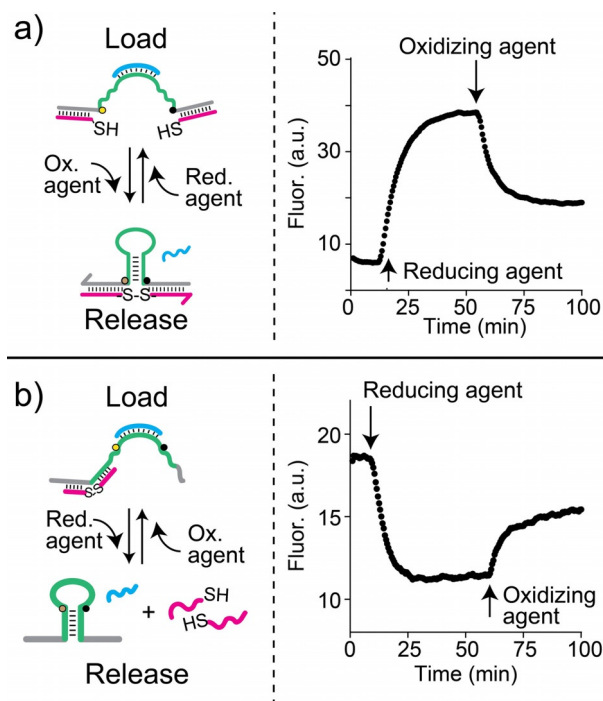

Figure 5. a) Reversible release and loading of the ligand $(5 \times 10^{-8}$ M) from the nanodevice $(3 \times 10^{-8}$ M) upon reduction and successive oxidation of the redox disulfide inhibitor $(3 \times 10^{-7}$ M). b) Reversible loading and release of the ligand $(3 \times 10^{-8}$ M) from the nanodevice $(3 \times 10^{-8}$ M) upon reduction and successive oxidation of the redox disulfide activator $(3 \times 10^{-7}$ M). Experiments were performed in 100 mM Tris-HCl, 150 mM NaCl, 10 mM $MgCl_2$ solution, pH 8.5, at 45°C. In both experiments, reduction was obtained by adding TCEP (final concentration: 3×10^{-3} M), while oxidation was obtained by adding H_2O_2 (final concentration: 1.5×10^{-2} M).

Conclusion

In conclusion, we have demonstrated here the rational design of a DNA nanodevice that can transiently load or release a DNA ligand upon the addition of a disulfide activator or inhibitor, under dissipative conditions. The system exhibits an unprecedented tolerance to waste products permitting reactivation of the system up to 40 times without a significant loss of efficiency in ligand-reloading kinetic. The redox transient kinetic of load and release of the ligand can be controlled by the rate with which the disulfide allosteric modulator is reduced to its thiolated halves. We have demonstrated that the approach is also reversible and allows to load and release a ligand upon successive reduction and oxidation of the modulator. These results demonstrate how the versatility, programmability and predictability of nucleic acid recognition make synthetic DNA/RNA the ideal material for designing non-equilibrium nanoscale systems. This is the first demonstration of a dissipative DNA-based ligand-binding nanodevice that relies entirely on chemical reactions rather than on DNA-recognizing enzymes. The advantages of this approach include a high tolerance against waste products, a more easily tunability of the kinetic response and a better stability of the system. Our approach paves the way to obtain chemically controlled transient regulation over a ligand-binding nanodevice, which could lead to more complex signalling pathways in synthetic mixtures.

Conflict of interest

The authors declare no conflict of interest.

[1] E. Mattia, S. Otto, *Nat. Nanotechnol.* **2015**, *10*, 111–119.
[2] B. A. Grzybowski, W. T. S. Huck, *Nat. Nanotechnol.* **2016**, *11*, 585–592.
[3] a) M. Fialkowski, K. J. M. Bishop, R. Klajn, S. K. Smoukov, C. J. Campbell, B. A. Grzybowski, *J. Phys. Chem. B* **2006**, *110*, 2482–2496; b) P. T. Corbett, J. Leclaire, L. Vial, K. R. West, J.-L. Wietor, J. K. M. Sanders, S. Otto, *Chem. Rev.* **2006**, *106*, 3652–3711.
[4] S. A. P. Van Rossum, M. Tena-Solsona, J. H. Van Esch, R. Eelkema, J. Boekhoven, *Chem. Soc. Rev.* **2017**, *46*, 5519–5535.
[5] F. Della Sala, S. Neri, S. Maiti, J. L. Y. Chen, L. J. Prins, *Curr. Opin. Biotechnol.* **2017**, *46*, 27–33.
[6] S. De, R. Klajn, *Adv. Mater.* **2018**, *30*, 1706750.
[7] G. Ragazzon, L. J. Prins, *Nat. Nanotechnol.* **2018**, *13*, 882–889.

[8] B. Rieß, R. Grötsch, J. Boekhoven, *Chem* **2020**, *6*, 552–578.

[9] R. Merindol, A. Walther, *Chem. Soc. Rev.* **2017**, *46*, 5588–5619.

[10] S. Mann, *Angew. Chem. Int. Ed.* **2008**, *47*, 5306–5320; *Angew. Chem.* **2008**, *120*, 5386–5401.

[11] E. Karsenti, *Nat. Rev. Mol. Cell Biol.* **2008**, *9*, 255–262.

[12] H. Hess, J. L. Ross, *Chem. Soc. Rev.* **2017**, *46*, 5570–5587.

[13] C. Pezzato, L. J. Prins, *Nat. Commun.* **2015**, *6*, 7790.

[14] S. Maiti, I. Fortunati, C. Ferrante, P. Scrimin, L. J. Prins, *Nat. Chem.* **2016**, *8*, 725–731.

[15] S. N. Semenov, A. S. Wong, R. M. van der Made, S. G. Postma, J. Groen, H. W. van Roekel, T. F. de Greef, W. T. Huck, *Nat. Chem.* **2015**, *7*, 160–165.

[16] S. Debnath, S. Roy, R. V. Ulijn, *J. Am. Chem. Soc.* **2013**, *135*, 16789–16792.

[17] C. Pezzato, C. Cheng, J. F. Stoddart, R. D. Astumian, *Chem. Soc. Rev.* **2017**, *46*, 5491–5507.

[18] C. Cheng, P. R. McGonigal, J. F. Stoddart, R. D. Astumian, *ACS Nano* **2015**, *9*, 8672–8688.

[19] a) S. Dhiman, K. Jalani, S. J. George, *ACS Appl. Mater. Interfaces* **2020**, *12*, 5259–5264; b) M. Malakoutikhah, J. J.-P. Peyralans, M. Colomb-Delsuc, H. Fanlo-Virgós, M. C. A. Stuart, S. Otto, *J. Am. Chem. Soc.* **2013**, *135*, 18406–18417.

[20] A. Jain, S. Dhiman, A. Dhayani, P. K. Vemula, S. J. George, *Nat. Commun.* **2019**, *10*, 450.

[21] C. Wanzke, A. Jussupow, F. Kohler, H. Dietz, V. R. I. Kaila, J. Boekhoven, *Mater. Horiz.* **2020**, *2*, e1900044.

[22] J. Boekhoven, A. M. Brizard, K. N. Kowlgi, G. J. Koper, R. Eelkema, J. H. van Esch, *Angew. Chem. Int. Ed.* **2010**, *49*, 4825–4828; *Angew. Chem.* **2010**, *122*, 4935–4938.

[23] A. K. Dambenieks, P. H. Q. Vu, T. M. Fyles, *Chem. Sci.* **2014**, *5*, 3396–3403.

[24] J. Boekhoven, W. Hendriksen, G. Koper, R. Eelkema, J. van Esch, *Science* **2015**, *349*, 1075–1079.

[25] C. S. Wood, C. Browne, D. M. Wood, J. R. Nitschke, *ACS Cent. Sci.* **2015**, *1*, 504–509.

[26] S. Dhiman, A. Jain, S. J. George, *Angew. Chem. Int. Ed.* **2017**, *56*, 1329–1333; *Angew. Chem.* **2017**, *129*, 1349–1353.

[27] S. Dhiman, A. Jain, M. Kumar, S. J. George, *J. Am. Chem. Soc.* **2017**, *139*, 16568–16575.

[28] N. Singh, B. Lainer, G. J. M. Formon, S. De Piccoli, T. M. Hermans, *J. Am. Chem. Soc.* **2020**, *142*, 4083–4087.

[29] A. Sorrenti, J. Leira-Iglesias, A. Sato, T. M. Hermans, *Nat. Commun.* **2017**, *8*, 15899.

[30] E. Del Grosso, A. Amodio, G. Ragazzon, L. J. Prins, F. Ricci, *Angew. Chem. Int. Ed.* **2018**, *57*, 10489–10493; *Angew. Chem.* **2018**, *130*, 10649–10653.

[31] E. Del Grosso, G. Ragazzon, L. Prins, F. Ricci, *Angew. Chem. Int. Ed.* **2019**, *58*, 5582–5586; *Angew. Chem.* **2019**, *131*, 5638–5642.

[32] L. Heinen, A. Walther, *Sci. Adv.* **2019**, *5*, eaaw0590.

[33] L. Heinen, A. Walther, *Chem. Sci.* **2017**, *8*, 4100–4107.

[34] J. Lloyd, C. H. Tran, K. Wadhwani, C. C. Samaniego, H. K. K. Subramanian, E. Franco, *ACS Synth. Biol.* **2018**, *7*, 30–37.

[35] S. Agarwal, E. Franco, *J. Am. Chem. Soc.* **2019**, *141*, 7831–7841.

[36] P. D. Ray, B.-W. Huang, Y. Tsuji, *Cell. Signalling* **2012**, *24*, 981–990.

[37] C. K. Sen, L. Packer, *FASEB J.* **1996**, *10*, 709–720.

[38] J. S. Stamler, *Cell* **1994**, *78*, 931–936.

[39] C. Abate, L. Patel, F. J. Rauscher III, T. Curran, *Science* **1990**, *249*, 1157–1161.

[40] E. Del Grosso, L. Prins, F. Ricci, *Angew. Chem. Int. Ed.* **2020**, https://doi.org/10.1002/anie.202002180; *Angew. Chem.* **2020**, https://doi.org/10.1002/ange.202002180.

[41] Y.-M. Go, D. P. Jones, *Crit. Rev. Biochem. Mol. Biol.* **2013**, *48*, 173–181.